Using the Critical Shoulder Angle as a proxy for the Acromion Index - A case study.

Bharath Narayanan[1] and Alexandre Terrier[1]

***Abstract*— In this project, I aim to establish whether the Critical Shoulder Angle (CSA) forms a good proxy for the Acromion Index (AI). Using the patient data that we have at the Laboratory of Biomechanical Orthopaedics at EPFL, I also aim to study if the CSA is a better indicator than AI, of Osteoarthritis (OA) and Cuff Tear Athropathy (CTA). I outline the various implementations I have made in order to automate the processes of scapula segmentation, glenoid extraction, and finally the measurements of the Acromion Index and the Critical Shoulder Angle.**

Using a dataset comprising 170 normal cases, 205 cases with OA, and 60 cases with CTA, I find that not only can CSA be used as a proxy for AI, it also demonstrates a larger size effect when comparing the means of the various data sets. I also find that the size effect of the CSA is more pronounced when identifying OA patients than it is when identifying CTA patients.

I. Introduction

Pathologies of the shoulder continue to impact the lives of patients around the world, specifically elderly patients. Two such pathologies are osteoarthritis (OA) and cuff tear arthropathy (CTA).

OA is a degenerative disease in which the cartilage in the joints wears down and sometimes bony growths called osteophytes develop in the joint. OA of the shoulder, while not being the most prevalent form of OA, has been found to affect almost 32.8 % [1] of adults over the age of 60 in the United States alone. It has also been found to reduce the functionality of the patients in terms of performing day to day tasks such as lifting objects or steering a car

CTA refers to the development of OA due to a rotator cuff tear (RCT). The rotator cuff is composed of four tendons which are attached to four muscles in the shoulder. The rotator cuff is tasked with ensuring that the shoulder remains stabilized in the 'socket' or glenoid. It enables us to move our arms outward and inward. When we raise our arms, the cuff slides between the humerus and the acromion and this causes the tendons to be 'pinched' or impinged, which can lead to their damage.

Over the course of many decades, attempts have been made to link the prevalence of rotator cuff tears and OA of the shoulder to the morphology of the scapula, specifically the acromion and the glenoid. The first classifications were qualitative in nature, such as the grouping of acromial shapes into three categories by Bigliani et al [2]. The three types were flat, curved and hooked and he posited that there were higher incidences of rotator cuff tears in patients with a hooked acromion. Following this, numerous attempts were made to obtain more quantitative parameters that could be used to measure the differences between various acromial shapes in a more substantial way.

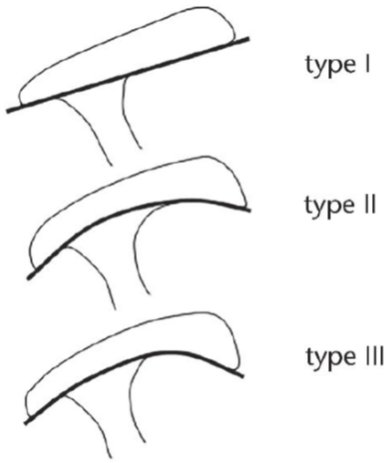

Fig. 1: The three types of acromial shapes, flat, curved, and hooked, as described by Bigliani et al. Image courtesy [7].

While studying radiographs of rotator cuff tears, Nyffeler et al found that the acromion appears large [4]. Hence they proposed a parameter to quantify the extent of this acromial extension by dividing the distance from the glenoid to the acromion by the distance from the glenoid to the most lateral part of the humeral head. They called this the acromion index (AI). Their study found an AI of 0.73 in patients with RCTs, 0.6 in patients with OA and 0.64 in a control group.

Later, Moor et al.[6] devised another method to classify the lateral extension of the acromion without involving the humeral head at all. They decided to measure the angle formed between the superior and inferior points on the glenoid and a line drawn from the inferior point on the glenoid to the most lateral point of the acromion. All of this was done on a standardised AP radiograph. They called this the critical shoulder angle (CSA). They found this angle to be on average 33.1 degrees in a control group, 38 degrees in RCT patients and 28.1 in patients with OA. Nyffler in another paper [7] also found that, when compared with the AI, the CSA differs more significantly between normal shoulders and shoulders with OA. This might be due to the fact that in shoulders with OA, the humeral head is flattened, giving rise to a higher AI. In addition to Nyffler, other studies including one by Blonna et al. [3] have shown

a strong link between CSA and the presence of OA.

The Laboratory of Biomechanical Orthopaedics has obtained, over the past few months, several CT scans of shoulders with and without pathologies. The primary pathology that is present in the dataset seems to be OA, with around 205 out of 291 scans. The second most prevalent pathology is CTA, with 60 cases. Instead of having a radiologist look at each radiograph manually, we have created a system that creates a 3D reconstruction of the scapula from which we can obtain the geometrical indicators automatically using Amira landmarks and snippets of code in Matlab. This is more efficient in the long run and less subject to observer biases. Currently, the only geometric parameter being measured is the AI. I would like to create a method to measure the CSA for each of the segmented scapulae and determine if it can be used as a proxy for the AI, and further, whether the CSA is a better indicator of OA than the AI.

A. Measures for categorizing geometries

While our scope is only limited to the AI and the CSA in this paper, I will provide a basic mention of a few other common measurements as well.

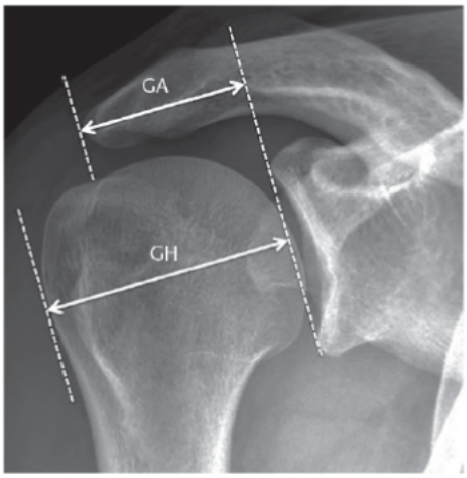

Fig. 2: The AI is the ratio of GA to GH. Image courtesy [7].

1) Acromion Index:

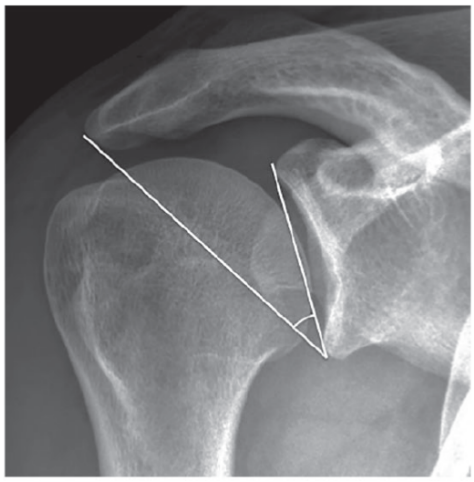

Fig. 3: The CSA is the angle shown in the figure. Image courtesy [7].

2) Critical Shoulder Angle: The CSA is the angle between the two lines connecting the Inferior and Superior Glenoid, and the Inferior Glenoid and the Acromial Lateral.

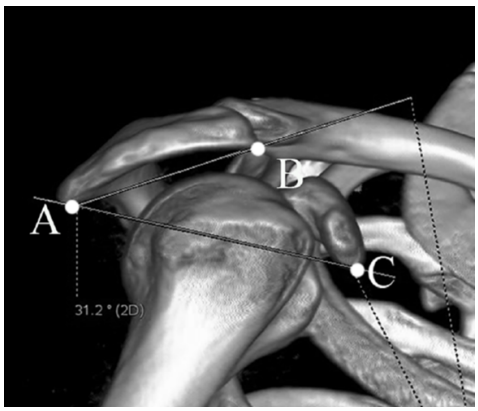

Fig. 4: The Acromial Tilt is the angle BAC. Image courtesy [5].

3) Acromial Tilt:

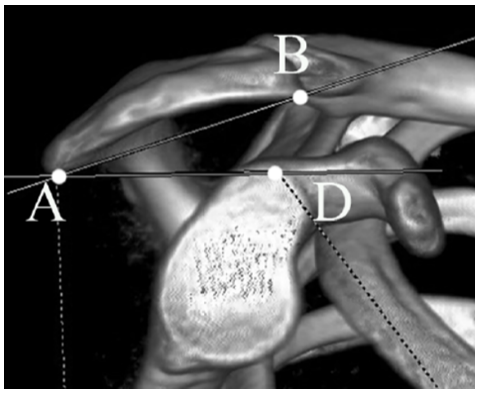

Fig. 5: The modified Acromial Tilt is the angle BAD. Image courtesy [5].

4) Modified Acromial Tilt: It might be worth trying to calculate the Modified Acromion Tilt in the future, especially, if we intend to have more pathological shoulders that have rotator cuff tears. It might need a bit more sophistication in detecting the most anterior and posterior points of the Acromion in the A-P plane but as Xinyu et al. have reported, it might be the optimal geometric parameter in terms of correlating with subacromial impingement [5].

II. Methods

In this section, I will cover a few aspects. One deals with the calculation of the AI and the CSA based on the geometry alone. After this, I will describe the automation of various scripts which allow us to generate the data found in the Results section. Finally, I will explain the statistical measurements we use to quantify the difference between the various datasets we have.

A. Measuring the Acromion Index

In order to measure the AI, all the scapula and glenoid points are projected onto the scapula plane, as shown in figure 6. We then identify the axis perpendicular to the scapular axis, passing through the inferior glenoid. This axis is then tilted such that it passes through the superior glenoid as well. The distance GA is measured from this new axis to the lateral most point of the acromion. GH is the distance of the lateral most point of the humeral head from the glenoid axis. We approximate GH using the diameter of the humeral head which is identified by using five manual landmarks. The different axes are shown in 7.

B. Measuring the Critical Shoulder Angle

In order to measure the CSA, we use the same projection of points onto the scapular plane as for the AI in figure 6. On this plane, the inferior glenoid (IG) and the superior glenoid (SG) are denoted by the most inferior and superior points of the glenoid in the I-S direction. The acromial lateral (AL) is the point on the acromion that is the furthest away from the body in the M-L plane. These points are outlined in the figure 8. Once these points are established, two vectors are created, connecting the IG and the SG, and the IG and the AL. The angle between them is calculated using the dot product rule.

$$\|\mathbf{A}\|\|\mathbf{B}\| cos\theta_{CSA} = \mathbf{A}^\top \mathbf{B}$$

After developing a method to calculate the CSA, I added the functionality to the current function that calculated the AI as well. This was stored in a file called $scapula\_calculation.m$. The previous code took as an input the location of the patient's files and loaded the scapula and glenoid points, both of which were identified manually. Both the scapula and glenoid were stored as stl files and were loaded as point clouds. The existing code already had a method for identifying the scapular plane and projecting all the glenoid and scapula points onto it. It also had a function for calculating the AI by first identifying the glenoid plane. From here on, I just needed to identify the inferior and superior glenoid points and the acromion lateral. This was done by simply using the matlab min and max commands in the correct directions. The new CSA measure was added to the outputted data structure called Result.

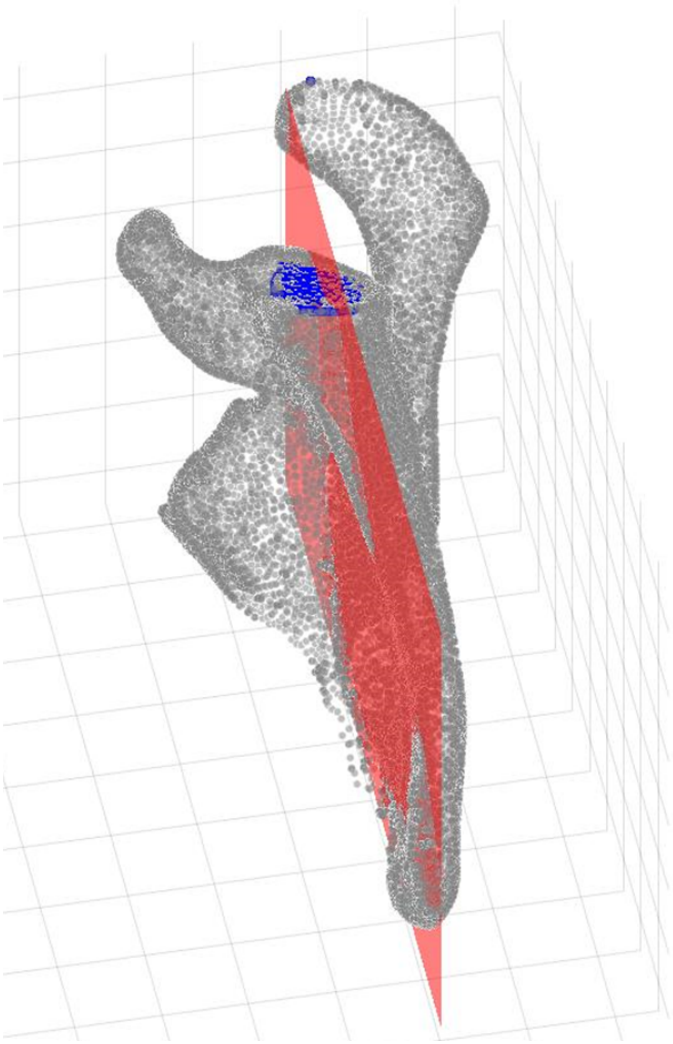

Fig. 6: This image shows the choice of the scapula plane onto which all the glenoid and scapula points will be projected. All the calculations used for determining the AI and the CSA will be based on vectors on this plane.

C. Automation of data collection

After having implemented the scapula calculation successfully, I then decided to create a new script to call the $scapula\_calculation.m$ file for each and every case for which the scapula and glenoid had been segmented. This involved a set of nested for loops and a check to make sure that the correct stl files were present. From the outputted Result data structure, I stored the AI and CSA values in two separate arrays. Once I had collected the AI and CSA from each segmented scapula, I then plotted the two together in Microsoft Excel using the scatter plot function.

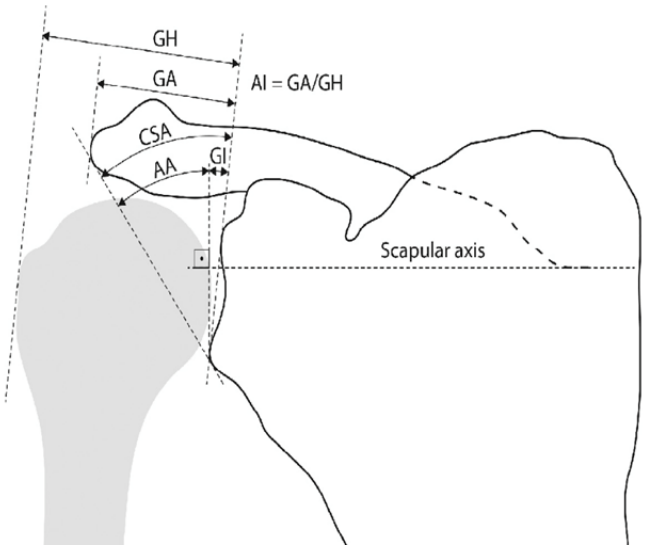

Fig. 7: This image shows the two dimensional scapula plane, glenoid and humeral head, with all the axes that are relevant. Note that the image has been taken from a presentation by Dr. Alex Terrier at the LBO.

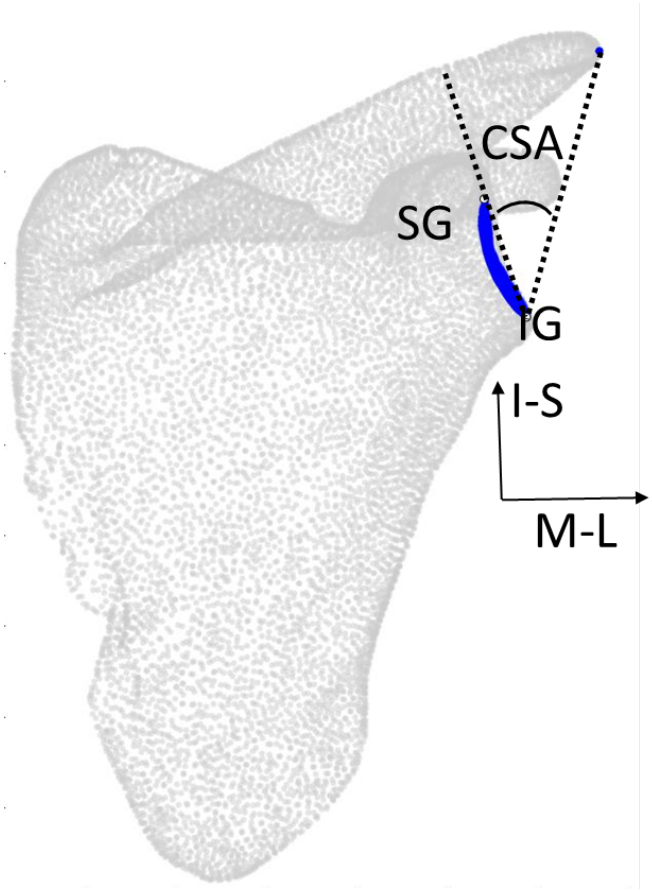

Fig. 8: This figure shows how the CSA is calculated. The points in this diagram are all the scapula points projected onto the scapula plane.

D. Automation of automatic scapula segmentation

The initial set of data, for which I could obtain the CSA and AI, consisted of only around 60 normal and pathological cases. In order to get more concrete results, I needed to obtain more data. Hence we decided to use the segmentation code developed in Berne to segment the scapula CTs automatically for all the normal and pathological cases. However, the code had to be run for each single case individually. In order to make things more efficient, we decided to automate the code and run it for all cases. Once again, this just consisted of nesting for loops and calling the right library functions which were provided to us by the developers. While running the automated code, we also took the decision to store the automatically segmented scapulae as ply files instead of stl files.

The automatic segmentation crashed a number of times for reasons that were unknown. In order to find out why this was happening and to report them to the developers, I needed to create a lot of 'try' and 'catch' segments. This would try a particular segment, for example, detecting the scapula side, and if the function call failed, it would store the failed patient ID and the reason for the failure. Using this data, we were able to report a few bugs which were then fixed by the developers.
In all, I was able to segment around 170 Normal datasets, including subnormal ones, and 291 Pathological datasets.

E. Automatic Glenoid Extraction

The next stage of my work involved the glenoid extraction procedure. The scapula segmentation in the previous code only segmented the scapula automatically. For the anatomical measurements, we not only need the scapula points but also the glenoid points. Thus far, the glenoid points were noted manually using landmarks that were stored in a text file, even when the scapula was being segmented automatically.

My task was to somehow extract the glenoid points from the automatically segmented scapula so that in future, the entire process could be automated. Fortunately, the developers at Berne had already provided the base code for me to work on. Their code to segment the scapula manually also called a function, $doMeasurements.m$ to perform certain glenoid landmark calculations and measurements. The function took in, as an input, the vertices and faces of all the scapula points. It then used these and some other algorithms to detect all the vertices of the scapula that formed the glenoid, before performing some landmark detection using these vertices. While I now had all the vertices of the glenoid, I also needed the faces, since you need both to create a new ply file that can be read by both Matlab and Amira for visualization. In order to obtain the faces, I did the following:

- I already had the faces of the scapula. I looped through each face which contains the indices of the 3 vertices that form the face.

Face	S.V.I. 1	S.V.I. 2	S.V.I. 3	G.V.I. 1	G.V.I. 2	G.V.I. 3
1	234	92	165	6	1	5
2	324	112	435	7	3	9
3	149	324	561	-	-	-
4	145	3125	298	-	-	-
5	1045	239	465	-	-	-

G.V.I.	S.V.I.
1	92
2	108
3	112
4	145
5	165
6	234
7	324

Fig. 9: Two tables that demonstrate the choice of face vertices. The table on the left shows how the face data is stored for the scapula and the glenoid. S.V.I. denotes the scapula vertex index and G.V.I. denotes the glenoid vertex index.

- If each of the 3 vertex indices of the current face was part of the glenoid vertex index subset, I counted this face as a face of the glenoid.
- This is not enough as I only have the vertex indices in the scapular frame of reference. I need to convert these into the glenoid frame by searching for the position of each of these face vertex indices in the set of vertices that consitute the glenoid. These are then returned as the vertex indices of the current glenoid face. An example is shown in figure 9. Here, scapula face 1 contains vertex indices 234, 92 and 165 in the scapula frame. We can see that all these vertices are also part of the glenoid subset. This means that scapula face 1 is also a face of the glenoid. However, when storing this face as part of the glenoid, we must use the glenoid indices which are taken from the table on the right.

Once the glenoid extraction has been done, the resultant file is stored as a ply file using the simplePlyWrite function that was developed by the programmers at Bern. The only task remaining was to loop through all the folders once again and then extract the glenoid from each of the existing scapula.

Note that initially, I did not store the glenoid as a set of vertices and faces. Instead, I had only stored the vertices which were then used to form a point cloud. This sufficed for all the matlab calculations but I realised that without information about the faces, it was not possible to visualize the automatically segmented glenoid in Amira. While this is not necessary for the moment, I felt it would be better to have the ability to visualize the glenoid in Amira as well.

F. Statistical Measures

In order to determine the importance of CSA or AI in distinguishing the pathologies from each other and from the normal cases, we need to turn to statistical measures. Two key parameters would be the p-value and the size effect.
The p-value tells us if the difference between the means of the various datasets is significant or not. In other words, a high p-value implies that the difference between the means can be attributed to variability in sampling rather than an actual tangible cause. As a corollary, a low p-value indicates that the difference in the means is significant.

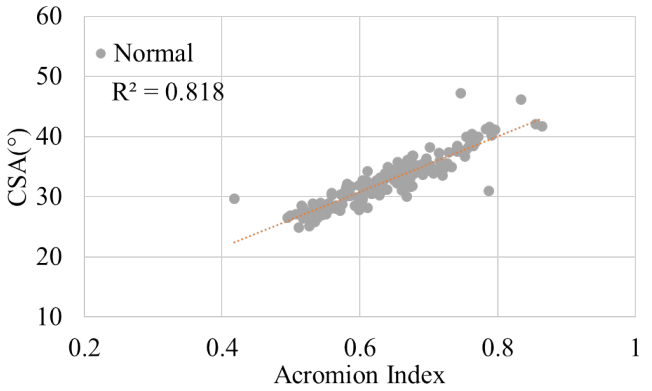

Fig. 10: AI vs CSA scatter plot for all normal data points, along with the R^2 value of the linear fit.

Once we know that there is a significant and real difference between the various datasets, we need to establish the size or the impact of the difference between their means. There are various ways to determine this, the simplest of which is to take the difference between the means and divide this by one of the two means. Over time, more sophisticated methods have been developed, the most well known being Cohen's D whose formula is outlined below.

$$Cohens_D = \frac{(\mu_2 - \mu_1)}{\sigma_{12}} \tag{1}$$

$$\sigma_{12} = \sqrt{\frac{\sigma_1^2 + \sigma_2^2}{2}} \tag{2}$$

μ is the mean of the dataset and σ is the standard deviation. A higher Cohen's D means that there is a larger size effect. For reference, a Cohen's d of 0.5 is a medium size effect, 0.8 is a large size effect, and 1.2 and over is a very large size effect.

III. Results

In order to obtain a relationship between the CSA and the AI, we loop through all the existing cases and calculate the CSA and AI. We then plot the results in figures 10, and 11. The scatter plots demonstrate high R^2 values of around 0.8. Figure 12 is used to focus on the OA and CTA cases alone. There is an observable shift of the CTA data to the top and to the right of the OA data.

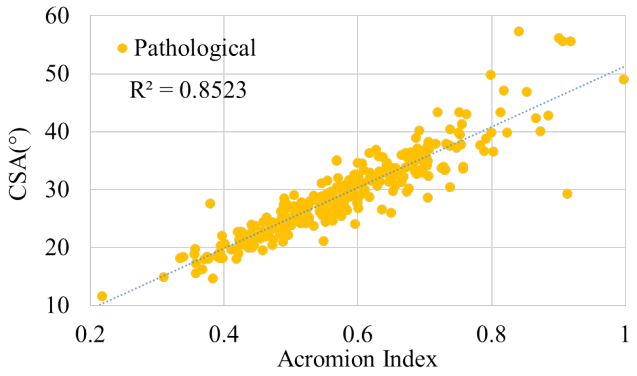

Fig. 11: AI vs CSA scatter plot for all pathological data points, along with the R^2 value of the linear fit.

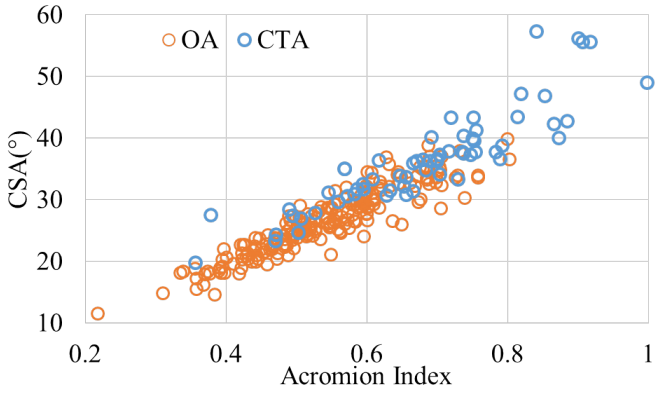

Fig. 12: Detailed CSA vs AI plot for the pathological dataset, showing only the OA and CTA cases. One can see a clear difference in the spread of the points for the two pathologies.

Figures 13 and 14 present the data in a more readable form. The crosses represent clear outliers of which there are a few, especially in the pathological datasets. The box plots show a slight overlap between the distributions of OA and CTA when using AI as a distinguishing factor and no overlap whatsoever when using CSA. For both the AI and the CSA plots, there is a clear difference in the median values for the normal, OA, and CTA cases, with the normal data falling between the OA and CTA cases. Visually, the spread or difference between the 25th and 75th percentiles (the top and bottom of the blue squares) seems lower in the CSA plot than in the AI plot. Figures 15 and 16 are used to outline the statistical findings and validation datasets respectively. It can be seen that the Cohen's D parameter is nearly double when using the CSA instead of the AI, for all three pairs of datasets. For both pairs involving OA data, the Cohen's D is well above 1. When the CTA data is paired up against the normal data, we get values that are lower than 1 standard deviation, even when using the CSA.

IV. Discussion

A. Linear fit

From figures 10 and 11, we can see a strong linear fit between the CSA and AI for both sets of data. There are

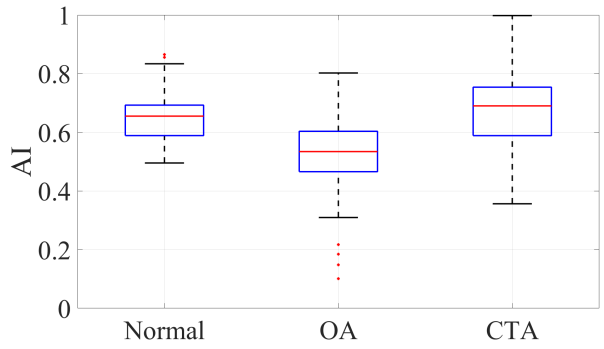

Fig. 13: A box plot that shows more clearly the difference in the median, and the 25th and 75th percentiles of the AI data for both, the normal, and the pathological data. The crosses denote the outliers.

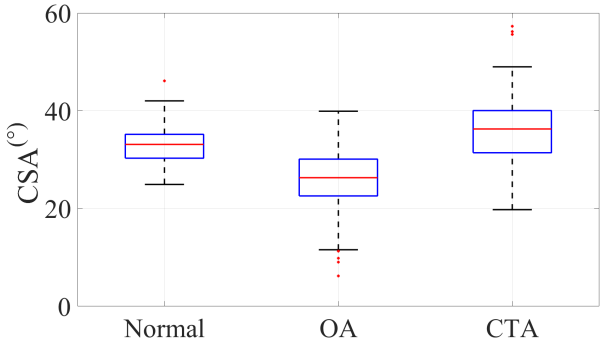

Fig. 14: A box plot that shows more clearly the difference in the median, and the 25th and 75th percentiles of the CSA data for both, the normal, and the pathological data. The crosses denote the outliers.

Cohen's D	CSA	AI
OA w CTA	1.59	0.84
OA w Normal	1.31	0.75
CTA w Normal	0.66	0.35

Fig. 15: Cohen's D for each combination of datasets. For all combinations, the size effect of CSA is almost double that of AI. The last row's values are notably lower for both CSA and AI. This could imply that the CSA is better used as an indicator for OA than it is for CTA.

CSA	Normal	OA	RCT/CTA
LBO	32.94	26.31	36.45
Moor	33.1	28.1	38.0
Ulrich	32.7	28.7	37.3
Bjarnison	33.3	31.1	33.9

Fig. 16: Validation of our data. Our data is compared with the values obtained by other researchers. Apart from Bjarnison et al, the others all find a significant difference among the 3 datasets.

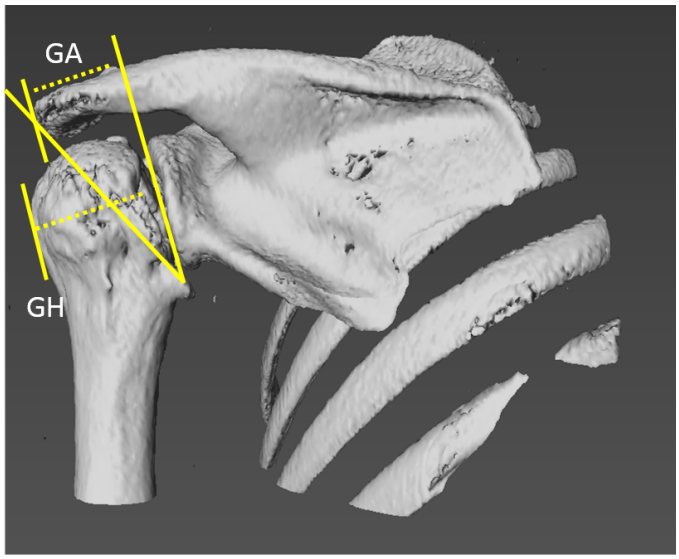

Fig. 17: An example of a case with a relatively high AI of 0.9, but a median CSA of 29.3. This shoulder has been observed to have avascular necrosis. The high AI here is due to the relatively flat humeral head. The sample is P274.

minor variations, however, especially when it comes to the pathological cases. This result is significant for us as a linear relationship generally implies that we can safely use the CSA as a proxy instead of AI.

B. Statistical findings

The p-value and the Cohen's D that we have calculated yield important information that allows us to make a definitive case for using the CSA instead of the AI. For all the pairs of data that we have presented, the p-value is well below 0.05, the threshold for significance. It is around 10^{-8}. The size effect when CSA is involved is around 1 standard deviation whereas for AI, it varies between 0.7 and 0.8 standard deviations. This is except for the comparison between the CTA cases and the normal cases, where the AI size effect drops to around .35 standard deviations while the CSA size effect drops to 0.66. From this, it can be inferred that CSA is better used as a distinguishing parameter for OA rather than for CTA even though the size effect for the CTA cases is still above the medium range.

C. Validation

Table 16 reaffirms the validity of our data. The CSA values we have found correspond well with those reported in literature by Moor, Ulrich and Bjarnison. In addition to this, independent manual observations by a radiologist at CHUV, Dr. Fabio Becce, also yield a mean CSA of 32.3 deg. The underlined row in the table refers to Bjarnisons's work. The relatively low difference between the normal and RCT groups led him to conclude that the CSA is better used for distinguishing OA than it is for distinguishing RCT. This resonates with our findings using the size effect results.

D. Avascular necrosis case

In figure 17, one can see an example of a case with high AI and a relatively average CSA. Having found certain data points that fall a distance outside of the expected linear fit in the CSA vs AI plot for pathological cases, I decided to visualize them and see if there was some erroneous data or whether there was a physiological reason for this. For this, I took P274 as an example and found that the humeral head is flattened. This causes the AI to be quite high. However, it does not impact the CSA since it is independent of the lateral most point of the humerus. This particular case had avascular necrosis which involves the death of bone cells due to the lack of sufficient blood supply.

E. Issues with automatic glenoid extraction

I have added figure 18 in order to demonstrate the shortcomings of the current automatic segmentation code. A cursory glance at the two sub-figures shows that the code segments the acromial protrusion fairly well. It is only when it comes to the glenoid region that it seems to have trouble. In this particular case, the reconstructed CT shows the glenoid and humerus touching each other as if they were almost one component. This could have confounded the segmentation code and resulted in the suboptimal segmentation shown in sub-figure (b).

V. Conclusion

The findings in the previous section lead me to conclude that it might be more prudent to use the CSA instead of the AI while trying to study pathologies in our dataset. The results of the comparison between the CSA and AI show that they form fairly reasonable proxies for each other. The CSA also demonstrates a larger size effect when comparing OA cases and CTA cases against the control group. In addition, the CSA can be measured completely using the automatic scapula segmentation (assuming it works 100 percent). However, for the AI, we also need to detect the humeral head and this is currently not part of the automatic segmentation code. Our findings regarding the higher effect size of CSA when compared with that of AI are also corroborated by other studies that have shown a greater correlation between CSA and OA than AI and OA. If anything, this only serves to strengthen our choice.

A. Improvements to the code

Currently, the work flow has been designed rather reactively. Now that we know how we would like the whole system to work, I believe that it is prudent to make sure that the glenoid identification as well as the measurements of the CSA and AI are done concurrently, along with the scapula segmentation routine.

For special cases for which the CT contains both, the right and the left scapulae, it makes sense to think of maybe accessing the patient database to find out which scapula side to segment. This will save us time.

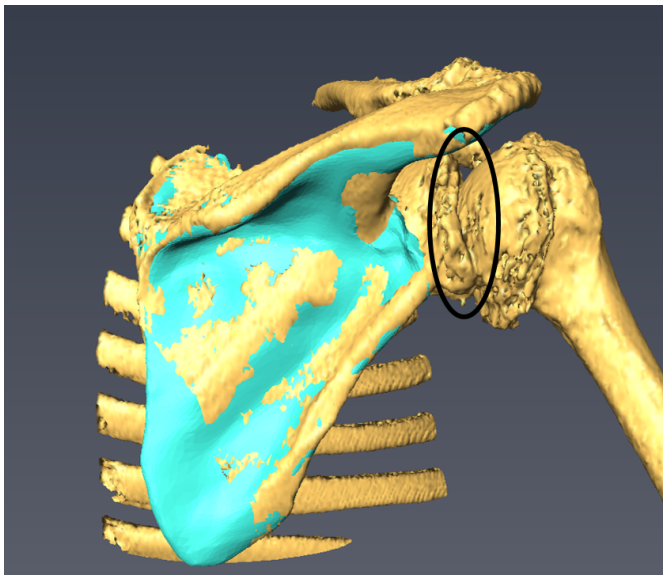

(a) The automatically segmented scapula superposed onto the actual 3D reconstruction of the CT using Amira.

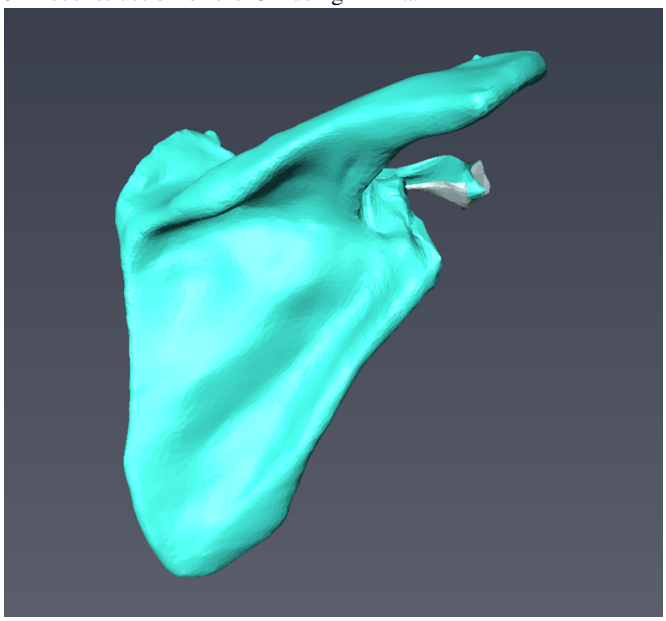

(b) The automatically segmented scapula only.

Fig. 18: This set of figures shows the shortcomings of the automatic glenoid extraction. It can be seen that the automatic scapula segmentation segments the acromion relatively well but struggles with the glenoid. As such, it can be used to determine the position of the acromion lateral fairly accurately. The poor glenoid segmentation could be due to the humerus being 'fused' with the glenoid, as shown in sub-figure (a). In sub-figure (b), the incomplete segmentation of the glenoid region can be seen more clearly.

B. New parameters

As mentioned earlier, I believe it might be worth taking a look at the modified Acromial Tilt. The calculation may be slightly involved but if there are more datapoints with rotator cuff tears then this might prove to be a better indicator than the CSA of such pathologies. In the study conducted in [5], the p-value of the mAT in predicting rotator cuff tears was the second lowest (0.0395) after Acromio-Humeral Index (AHI). Unlike the AHI, however, the mAT needs, once again, only the segmented acromion and glenoid components which we already have.

VI. Acknowledgements

I would like to thank Dr. Alex Terrier and Jorge Solana Munoz for their continued support during my semester project. Alex was always available when I needed him, especially in matters concerning Amira. Jorge took active interest in my project and proactively came up with quite a few suggestions which were extremely helpful.

References

[1] Centers for Disease Control and Prevention (CDC), Prevalence and most common causes of disability among adultsUnited States, 2005. Morbidity and Mortality Weekly Report (MMWR) (2009); 58(16):421426.

[2] Bigliani LU, Morrison DS, April EW. The morphology of the acromion and its relationship to rotator cuff tears, Orthop Trans (1986) ;10:216.

[3] Blonna D., Giani A. et al, Predominance of the critical shoulder angle in the pathogenesis of degenerative diseases of the shoulder, Journal of Shoulder and Elbow Surgery, (Aug 2016), p. 1328-36.

[4] Nyffeler RW, Werner CM, Sukthankar A, Schmid MR, Gerber C. Association of a large lateral extension of the acromion with rotator cuff tears. J Bone Joint Surg [Am] (2006) ;88-A:800-805.

[5] Xinyu Li et al, Relationship between acromial morphological variation and subacromial impingement: A three-dimensional analysis., PLOS One 25/04/2017

[6] Moor BK, Bouaicha S, Rothenfluh DA, Sukthankar A, Gerber C. Is there an association between the individual anatomy of the scapula and the development of rotator cuff tears or osteoarthritis of the glenohumeral joint? A radiological study of the critical shoulder angle. Bone Joint J (2013) ;95-B:935-941.

[7] Nyffler RW, Meyer DC. Acromion and glenoid shape: Why are they important predictive factors for the future of our shoulders?, Instructional Lecture, Shoulder and Elbow, EOR Volume 2 May (2017)

[8] Arnar Bjarnison, TJ. Srensen, T Kallemose, KW Barfod. The critical shoulder angle is associated withosteoarthritis in the shoulder but not rotator cufftears: a retrospective case-control study, J Shoulder Elbow Surg (2017) 26, 20972102

[9] Ulrich JS et al. The critical shoulder angle is associated with rotator cuff tears and shoulder osteoarthritis and is better assessed with radiographs over MRI, Knee Surg Sports Traumatol Arthrosc (2016) 24:22442251

VII. Appendix A

This appendix runs through the current workflow. All files and folders are located in the lbovenus.epfl.ch server under the shoulder directory. There are 3 broad parts which can be run separately from each other:

- Scapula Segmentation
- Glenoid Extraction
- CSA and AI Measurements

A. Scapula Segmentation

The segmentation of the scapula can be done either manually, by logging into Amira and then choosing the landmarks or automatically, using the code developed at Berne. For my part, I have only outlined how the automatic segmentation is done.

- Run

  `methods\matlab\segmentation\method\howToPrepareData_BN.m`

  using putty on the lbovenus server itself. The command is provided in the matlab file as a comment.
- There are two modes of operation:
  - Go through each patient in each folder. This is the default if no input is provided. Only restriction is that you have to choose if your data is normal or pathological.
  - Provide a list as an input with different patient IDs e.g.

    ```
    list = {'P254';'P275'}
    ```
- It generally takes around 15 minutes to segment 1 case. At the end of the case, the segmented scapula is saved as a .ply file in the respective folder. In addition to this, there might be measurements done which are then stored as a matlab database. An example is shown below:
  - `data\N\2\1\N211-473370\CT-N211-473370-1\matlab\auto\scapulaSurfaceAuto.ply`
  - `data\N\2\1\N211-473370\CT-N211-473370-1\matlab\auto\anatData`

Note that the measurements mentioned above only detect and calculate landmarks and not parameters such as the AI or CSA.

B. Glenoid extraction

Once the scapula has been segmented, the glenoid points need to be identified. When the scapula has been extracted manually, the glenoid can only be identified manually using a set of landmarks stored as an ASCII text file. However, when the scapula has been segmented automatically using the code from Berne, we have a choice between identifying (or extracting) the glenoid manually or automatically. The following are some general pointers in the use of the automatic glenoid segmentation algorithm.

- I used parts of Elhaam's code to create the glenoid extraction function :

  `methods\matlab\segmentation\method\extractGlenoidSurface.m`
- Initially, I only used her code to obtain the vertices of the scapula that formed part of the glenoid. While this was sufficient to create a point cloud in matlab (for calculation purposes), it rendered the extracted glenoid surface un-viewable in Amira. This is because Amira needs both faces and vertices in order to process a surface.
- I solved this by looping through all the faces of the scapula and detecting those faces that contained vertices which were all part of the glenoid vertex subset. Note that the face information needs to contain the local glenoid vertex indices for which minor manipulations were required. Now, the glenoid ply file contains face and vertex information.
- We had decided to do the automatic glenoid identification after all the scapulae were segmented automatically. In order to not run the scapula segmentation code again, I created the following function to loop through all the existing scapula ply files and extract the glenoid from them:

  `methods\matlab\segmentation\method\extractAllGlenoid.m`
- For each scapula, the function extracts all the glenoid points and stores them in another ply file called

  `data\N\1\1\N110-134379\CT-N110-134379-1\matlab\auto\glenoidSurfaceAuto.ply`
- In future, the glenoid identification will be integrated with the scapula segmentation code so that for all new cases, the glenoid identification is done immediately after the scapula has been segmented.

So far the automatic glenoid identification does not seem to work as well as we would like. The hope is that in future, we would be able to avoid all manual tasks as far as possible. Until then, we use the manually segmented glenoid surface stored as a .stl file:

`data\N\1\1\N110-134379\CT-N110-134379-1\amira\ExtractedSurfaceN110.stl`

VIII. Calculating the CSA

Once the scapula and glenoid have been identified, the essential measurements are conducted.

- Currently, there are two sets of measurements. One has been done by Elhaam. This is stored as

  `methods\matlab\segmentation\method\doMeasurements.m`

  This function is called automatically during the automatic segmentation of the scapula. Note that this function only calculates landmarks and measures the glenoid

properties such as its radius. It does not calculate the CSA or AI or any other such index.

- The other has been done in-house. It has been edited by a number of people including Bharath and Killian. It is stored as

  `methods\matlab\segmentation\method\scapula_calculation_ply_glenoidAuto.m`

  , and

  `methods\matlab\segmentation\method\scapula_calculation_ply_glenoidManual.m`

  and

  `methods\matlab\segmentation\method\scapula_calculation.m`

  - For the third function, the scapula is inputted as a .stl file. For the other two, the scapula is inputted as a .ply file but the glenoid used is either manually (input is a .stl file) or automatically segmented (input is a .ply file).
  - For all these files, the only inputs are the **location**, either 'N' for normal, or 'P' for pathological, the **subject**, e.g. 'N110-134379', and the **directory**, e.g.

    `data\N\1\1\`

- Currently, the measurements done in-house are not done simultaneously along with the scapula segmentation.
- Instead, once all the scapulae have been segmented, we run the following code to loop through each patient ID to perform the measurements on each segmented scapula and glenoid combination that is present:

  `methods\matlab\segmentation\method\getAllRecords_ply.m`

  As the function name suggests, it uses only ply files as input for the scapula i.e. it only uses the automatically segmented scapulae as inputs.
- The results of the measurements are currently not stored as a database but this is an aim which we have. In addition to saving the data, we will also work to ensure that the measurements are conducted along with the scapula segmentation.